All-Optical Analog to Electromagnetically Induced Transparency in Multiple Coupled Photonic Crystal Cavities

Xiaodong Yang,[1,*] Mingbin Yu,[2] Dim-Lee Kwong,[2] and Chee Wei Wong[1,†]

[1]*Optical Nanostructures Laboratory, Center for Integrated Science and Engineering, Solid-State Science and Engineering, and Mechanical Engineering, Columbia University, New York, New York 10027, USA*

[2]*The Institute of Microelectronics, 11 Science Park Road, Singapore 117685, Singapore*

(Received 11 October 2008; revised manuscript received 2 February 2009; published 30 April 2009)

We report first observations of deterministic phase- and resonance-controlled all-optical electromagnetically induced transparency in multiple coupled photonic crystal cavities. The full-range tuning of coherently coupled cavity-cavity phase and resonances allow observations of transparency resonance in dark states with lifetimes longer than incoherently summed individual cavities. Supported by theoretical analyses, our multipump beam approach allows arbitrary control in two and three coupled cavities, while the standing-wave wavelength-scale photon localization allows direct scalability for chip-scale optical pulse trapping and coupled-cavity QED.

DOI: 10.1103/PhysRevLett.102.173902 PACS numbers: 42.60.Da, 42.50.Gy, 42.70.Qs, 42.82.−m

Quantum coherence in atomic systems has led to fascinating and counterintuitive outcomes, such as laser cooling, trapping of atoms, and Bose-Einstein condensates. In electromagnetically induced transparency (EIT), the quantum destructive interference between excitation pathways to the upper level in three-level atomic systems has led to a sharp cancellation of absorption in the medium [1], resulting in phenomena such as lasing without inversion and freezing light [2], and dynamical storage of light in a solid-state system [3]. It has been shown that N-2 areas of EIT transparency windows with low absorption will be created in N-level atomic systems, supporting slow group velocities for N-2 probe pulses at different frequencies, which can be used for efficient quantum entanglement generation and nonlinear optical processes [4].

Similar to atomic systems, where the interference is driven by a coherent laser field, EIT-like effects can be observed through classical means [5]. Particularly, coherent interference between resonant modes induces the absence of absorption in coupled optical resonators. Several theoretical proposals have suggested this intriguing possibility in an optical analogy to atomic EIT [6–8], overcoming much of the limitations on decoherence and bandwidth from electronic states for EIT, with applications in stopping light and trapping light at room temperature [6]. Slow light in photonic structures has been examined [9] but is likewise bounded by the fundamental delay-bandwidth limit. Recently EIT-like effects were examined experimentally in two coupled whispering-gallery mode resonators [10,11], storing light on-chip beyond the static bandwidth limit. These are, however, large traveling-wave resonators of $\sim 10(\lambda/n)^3$ or more modal volumes, with arbitrary azimuthal modes. Moreover, simultaneous phase control in the interference pathways has never been achieved, and the interactions have been limited to only two resonators.

Here we present experimental observations of all-optical EIT in multiple standing-wave photonic crystal cavities, with deterministic *phase* and *resonance* tuning. Not only are the cavities with the fundamental mode and modal volumes at $\sim(\lambda/n)^3$, but in the three cavity regime, demonstrates multiple EIT-like line shapes.

The system (Fig. 1) consists of a photonic crystal waveguide side-coupled to two and three high intrinsic quality factor (Q) photonic crystal cavities [6,12]. These defect-type cavities, with three missing air holes ($L3$) in a triangular-lattice photonic crystal membrane (0.29a hole radius, 0.6a thickness lattice, lattice period a of 420 nm), allow wavelength-scale localization [modal volume $V \sim 0.74(\lambda/n)^3$] with ultrahigh Q factors [13] for nonlinear [14] and quantum optics. Each cavity has S_1 tuned for increased intrinsic Q factors Q_{int} at ~60 000 [13], calculated from three-dimensional finite-difference time domain [15]. The waveguide-cavity coupling Q_c is ~1600, for a total Q_{tot} of 1560. In this work, we deliberately achieved Q_{int}/Q_c to be high (~37.5) in each cavity, to operate in the strongly overcoupled regime for in-plane interference. When two cavity resonances, ω_1 and ω_2, overlap [with $\delta_{12} = 2\tau_{\text{total}}(\omega_1 - \omega_2) \neq 0$, where τ_{total} is the loaded lifetime of single cavity] and the cavity-cavity round-trip phase 2ϕ satisfy the condition of a Fabry-Perot resonance ($2n\pi$), the system thereby represents an all-optical analogue of EIT, with two degenerate modes at $(\omega_1 + \omega_2)/2$. From coupled-mode analysis, when $\delta < \sim 3.5$, $Q_{\text{EIT}} > Q_{\text{total}}$, satisfying the condition of EIT-like coherent interference. Figure 1(b) shows the transparency mode distribution in the dark state of two coupled $L3$ cavities. Of the two degenerate modes, the mode with decay slower than a single cavity lifetime gives rise to the EIT-like spectral feature [16]. We generalize the concept of all-optical EIT from two coupled resonators to multiple EIT-like transmission with N coupled resonators [8], for unique line

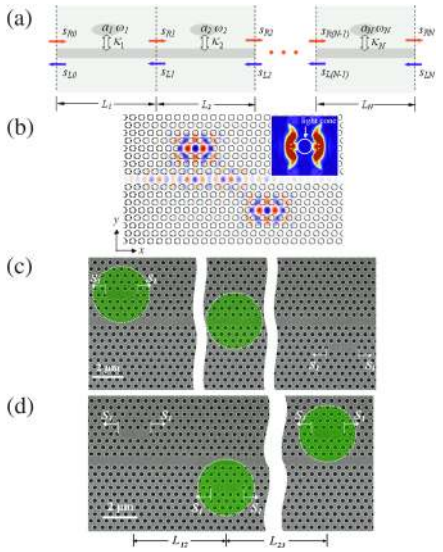

FIG. 1 (color online). (a) Schematic of multiple EIT-like system including a central waveguide side-coupled to N cavities. (b) E_y field intensity of coupled-cavity transparency mode between two $L3$ cavities. Inset: k-space amplitudes for single $L3$ cavity, illustrating high intrinsic Q. (c) SEM of two-$L3$-cavity system, with phase detuning between the cavities. Each cavity is tuned ($S_1 = 0.15a$) for high intrinsic Q. (d) Multiple EIT-like system with three $L3$ cavities. The green spots indicate the focused pump beams used for thermo-optic tuning.

shapes and coupled-cavity QED [17]. Figure 1(d) shows the multiple EIT-like system, consisting of three coupled cavities with separation $L_{12} = 12a$, and $L_{23} = 30a$.

The devices are fabricated in a silicon-on-insulator substrate, with 248-nm deep-UV lithography. The scanning electron micrograph (SEM) in Fig. 1(c) shows an example structure studied, where the statistically parametrized [18] fabrication disorder shows a small edge roughness and correlation length of 1.66 and 18 nm, respectively. The lattice period is bounded within 422.97 ± 1.65 nm, with hole radius of 121.34 ± 1.56 nm and feature ellipticity of 1.57 ± 0.79 nm. The single-crystal device layer is 250 nm thick, on top of a sacrificially etched 1 μm buried oxide. Tapered lensed fibers with in-line fiber polarization controllers couple transverse-electric light from an amplified spontaneous emission source, with optical spectrum analyzer detection. To align the cavity resonances and the multicavity phases, instead of a recent digital tuning method [19], here we use a thermo-optic method to tune both δ and ϕ simultaneously. Two 532 nm continuous-wave lasers are locked to a 5 μm spot size at either both cavity regions or a cavity and interconnecting waveguide region [Fig. 1(c)] for local perturbations. With dn/dT of 1.85×10^{-4}/K at 300 K, we estimate ~16 K temperature rise per milliwatt pump. Pump positions and powers are carefully selected to precisely control both δ and ϕ for each coherent interference state.

We present four example series of experiments: the first (Fig. 2) with two coupled cavities initially mismatched and without phase control; the second [Figs. 3(a)] with two coupled cavities initially resonance matched and without phase control; the third [Figs. 3(b)] with simultaneous phase and resonance tuning of two coupled cavities; the fourth (Fig. 4) with three coupled cavities for multiple EIT-like interferences. In Figs. 2(a), the black, solid curves illustrate the measured transmission spectra of the EIT-like photonic crystal system under various pump powers for sample 1. Figure (2a.i) shows the initial transmission for two uncoupled standing-wave cavities, with two separated Lorentzian line shapes, with resonances $\lambda_1 = 1548.63$ nm and $\lambda_2 = 1549.45$ nm. With increased pump power, both cavity resonances are redshifted (linear, with ~1.32 nm per mW pump) and the detuning deterministically narrower. When the pump power is 0.28 mW, the detuning δ is 2.74, and an EIT-like transparency peak distinctively appears. With further decrease in detuning δ, the transparency peak progressively narrows, supporting

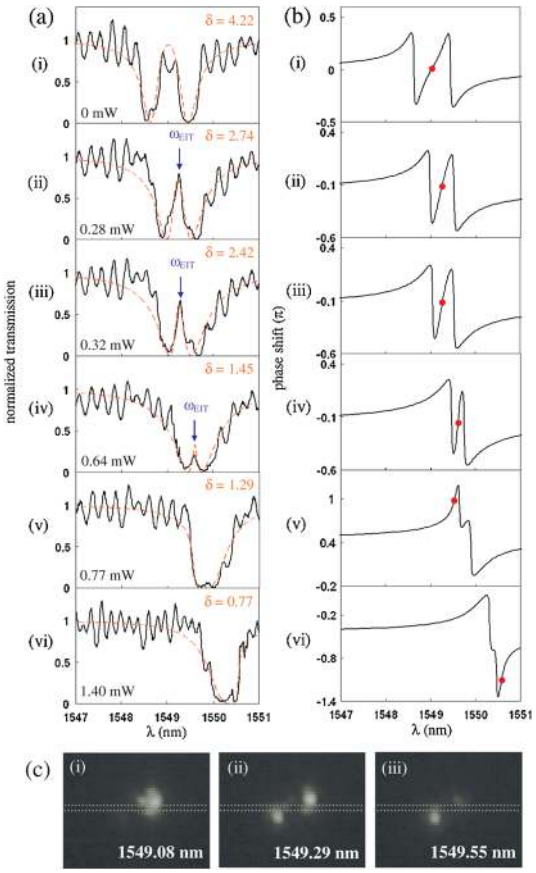

FIG. 2 (color online). (a) Measured and theoretical transmission line shapes with various detuning δ for sample 1. Center-to-center separation $L = 11a$. Solid black lines show experimental data and red dashed lines show theoretical fits. (b) Corresponding theoretical transmission phase shift. The red dots show the locations of EIT-like peaks, or Fano-like transitions where the phase slope is positive and steepest. (c) Top-collected radiation images of the light emitted from the defect region with conditions illustrated in (a.iii). The superimposed gray dotted lines depict the same position of the photonic crystal waveguide.

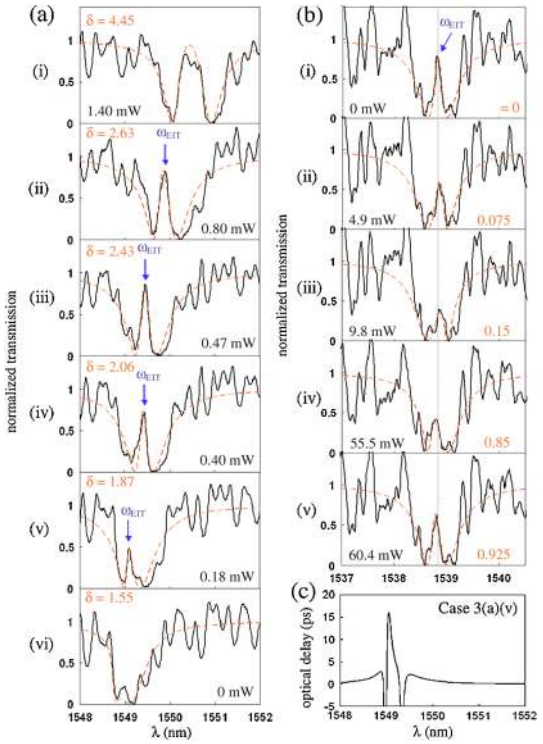

FIG. 3 (color online). (a) Measured and theoretical transmission line shapes with various detuning δ for sample 2, $L = 10a$. (b) Measured and theoretical transmission line shapes with various phase difference $\Delta\phi$ at $\delta = 1.92$ for sample 3, $L = 142a$. The dotted gray lines show the position of the EIT-like transparence peak for $\Delta\phi = 0$. (c) Calculated optical delay.

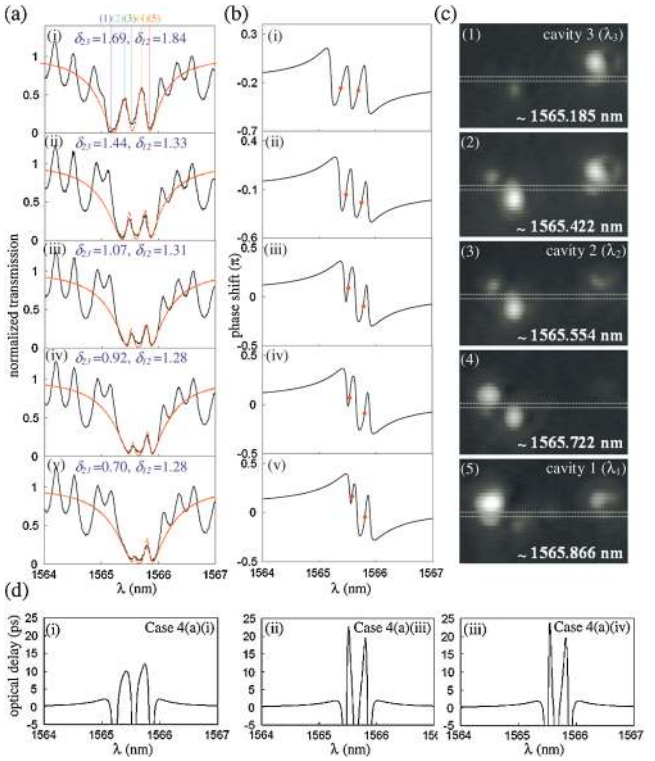

FIG. 4 (color online). (a) Measured and theoretical transmission line shapes with various detuning δ_{12} and δ_{23} for sample 4. (a.i) Denotes the frequencies where the radiation images are collected. (b) Corresponding theoretical transmission phase shift. (c) Top-collected radiation images for various detunings. (d) Calculated optical delays for double EIT-like peaks.

increased interference between the two cavity modes. The FWHM of the symmetric transparency peak in Fig. (2a.iv) is 120 pm, or a Q_{EIT} of 13 000, sizably larger than Q_{tot} of *each* $L3$ cavity and a longer photon delay than two noninteracting cavity lifetimes combined. For the single cavity, the measured linewidths have $Q_{\mathrm{tot},1} \sim 4000$ and $Q_{\mathrm{tot},2} \sim 3600$, and Q_{int} is ~60 000 as estimated from the ~22.5-dB transmission dips.

Under stronger pump excitation, Figs. (2a.v) and (2a.vi) now show Fano-like line shapes (due to $\phi \neq n\pi$), with the highly asymmetric (sharp on or off transmission) edge shifting from the blue to the red edge. We emphasize that only the unprocessed measurement data are shown, where the Fabry-Perot noise oscillations (~ 2.5-dB contrast versus the EIT-like peak with ~22.5-dB intensity contrast) are due to waveguide end facet reflections, removable with a fiber-to-chip mode converter. In Figs. 2(c), we verified the mode field distributions under controlled tuning. At each cavity resonance, the radiation exhibits a single bright mode with fundamental even symmetry. In contrast, exactly at the EIT-like transparency peak, both cavities can be imaged together, confirming coherent interference of the two coupled cavities.

Sample 2 now shows two cavities with initial small detuning (approximately the single cavity linewidth), with resonances at 1549.10 and 1548.80 nm, and measured $Q_{\mathrm{tot},1} \sim 4100$ and $Q_{\mathrm{tot},2} \sim 3100$, respectively. Without any external pumping, the transmission already shows asymmetric Fano-like line shapes [Fig. 3(a.vi)]. Upon pump tuning, the two cavity resonances *separate* and the strong in-plane coherent coupling results in clear observations of the EIT-like line shapes [Figs. 3(a.ii)–3(a.v)]. The FWHM of the transparency peak in Fig. 3(a.v) is ~150 pm, or a Q_{EIT} of 10 400.

In the third series of experiments, in order to control the cavity-cavity detuning δ *and* phase difference ϕ independently with two pump beams, the in-plane separation of two cavities is designed to be $L = 142a$, or $\cong 60\ \mu$m [sample 3, Fig. 1(c)]. The initial resonance are 1535.80 and 1539.01 nm, with measured $Q_{\mathrm{tot},1}$ and $Q_{\mathrm{tot},2} \sim 4000$. The two pump beams are aligned with one at cavity 1 to perturb the resonance and the other at the interconnecting waveguide to tune the phase ϕ. First, the pump power of the first laser is adjusted to decrease detuning δ from 16.69 to 1.92 and reach the optical EIT-like regime ($\delta < \sim 3.5$), where the tuned $\lambda_1 = 1538.64$ nm and λ_2 does not change. Next, the second laser pump intensity is tuned to control the round-trip phase 2ϕ. When 2ϕ is close to $2n\pi$, a narrow and symmetric EIT-like peak is seen [Fig. 3(b.i)], with FWHM ~160 pm, or a Q_{EIT} of 9600. The phase shift $\Delta\phi$ per mW pump power is linear and $\sim 0.0153\pi$/mW. $\Delta\phi$ is deterministically controlled between the full range

of 0 to π. When $\Delta\phi \neq 0$ and less than 0.5π, each line shape is asymmetric and red-tilted, and the center peak broadened with lower transmission. Both cavity resonances are not shifted, indicating independent δ and ϕ control have now been achieved. As $\Delta\phi$ is increased above 0.5π, the transparency appears again with blue tilt [Figs. 3(b.iv) and 3(b.v)].

The multiple EIT-like transmission is then demonstrated with three cavities (sample 4). The initial resonances for three cavities are around 1565 nm with $\lambda_1 > \lambda_2 > \lambda_3$. As in Fig. 1(d), the two pump beams are focused on cavities 2 and 3 to perturb λ_2 and λ_3, respectively. In Figs. 4(a), the black solid curves illustrate, for the first time, the measured transmission spectra of the multiple EIT-like photonic crystal system under various pump powers. We emphasize that these are cases for the three cavities interacting altogether to allow these line shapes. Initially, the pump powers of two beams are tuned to control detuning δ_{12} and δ_{23} to reach the multiple EIT regime ($\delta_{12} = 1.84$ and $\delta_{23} = 1.69$) [Fig. 4(a.i)], where double EIT-like transparency peaks distinctively appear. Pump power of the second laser is next increased so that λ_3 is continually redshifted and the resonance detuning δ_{23} is decreased. As shown in Figs. 4(a.ii)–4(a.v), the transparency peak between cavities 2 and 3 progressively narrows, indicating stronger interference between these two cavities among the three cavity interferences. The FWHM of the two transparency peaks in Fig. 4(a.iv) are ~74 and ~95 pm, respectively, corresponding to Q_{EIT} of ~21 100 and ~16 500. The phase shift is close to zero in Fig. 4(a.iv) and hence the twin EIT-like linewidths are narrower than earlier measurements; in Figs. 4(a) any asymmetric line shape is due to $\phi \neq n\pi$. Figures 4(c) further shows the radiation images for case 4(a.i), with largest detuning for imaging.

All four example series of measured EIT-like line shapes are examined with the coupled-mode formalism [20], with theoretical model in Fig. 1(a). The dynamical equation for the multicavity mode amplitudes is $\frac{da_N}{dt} = [-(1/2\tau_{\mathrm{total},N}) + i(\omega_N + \Delta\omega_N - \omega_{\mathrm{wg}})]a_N + \kappa s_{R,(N-1)} + \kappa s_{L,N}$, where N denotes the cavity number, a the cavity mode amplitude, and s the waveguide mode, with $s_{L,(N-1)} = \exp(-i\phi)s_{L,N} + \kappa a_N$ and $s_{R,N} = \exp(-i\phi)s_{R,(N-1)} + \kappa a_N$ [14]. $\phi = \omega_{\mathrm{wg}} n_{\mathrm{eff}} L/c$ is the multicavity phase difference, with waveguide mode index n_{eff} of 2.768 at 1.55 μm. κ is the coupling coefficient between s and a, and $\kappa = i\exp(-i\phi/2)/\sqrt{2\tau_c}$. The total loss rate for the cavity mode $1/\tau_{\mathrm{total}}$ is $1/\tau_{\mathrm{total}} = 1/\tau_c + 1/\tau_{\mathrm{int}}$, with $1/\tau_c$ ($= \omega/Q_c$) and $1/\tau_{\mathrm{int}}$ ($= \omega/Q_{\mathrm{int}}$) the cavity decay rates into the waveguide and continuum, respectively. Solving the transmission $T = |s_{2-}|^2/|s_{1+}|^2$ numerically, the red dashed curves in Figs. 2(a), 3(a), 3(b), and 4(a) all show remarkable theoretical fits to the four series of experiments, with only one (ϕ) fitting parameter. Figures 2(b) and 4(b) show the corresponding phase shifts with steep dispersions, with the single and multiple EIT-like transparencies. The calculated optical delays are shown in Figs. 3(c) and 4(d); for example, the double EIT-like peaks in Fig. 4(d.i) have optical delays of 9.8 and 11.9 ps. With stronger coupling between cavities, Fig. 4(d.ii) now gives optical delays of 22.5 and 19.2 ps at two EIT-like peaks.

In summary, we demonstrate experimentally the deterministic tuning of all-optical multiple EIT in multilevel coherently coupled cavities, with both phase- and resonance-tuning control. In our photonic crystal cavities with wavelength-scale localization, distinctive EIT-like and Fano-like line shapes are observed, with measured EIT-like linewidths narrower than individual resonances. Our experimental and theoretical results support efforts towards realization of photon pulse trapping, dynamic bandwidth compression, and coupled-cavity QED in scalable photonic crystal cavity arrays.

The authors acknowledge support by DARPA, NSF, and Intel (X. Y.). We are particularly grateful for the review comments for further motivating new studies and results.

*xy2103@columbia.edu
†cww2104@columbia.edu

[1] S. E. Harris, Phys. Today **50**, No. 7, 36 (1997).
[2] S. E. Harris, Phys. Rev. Lett. **62**, 1033 (1989); L. V. Hau *et al.*, Nature (London) **397**, 594 (1999).
[3] J. J. Longdell *et al.*, Phys. Rev. Lett. **95**, 063601 (2005).
[4] M. D. Lukin and A. Imamoglu, Phys. Rev. Lett. **84**, 1419 (2000); L. Deng *et al.*, Phys. Rev. Lett. **88**, 143902 (2002); D. McGloin *et al.*, Opt. Commun. **190**, 221 (2001); J. Wang *et al.*, Phys. Lett. A **328**, 437 (2004).
[5] G. L. Garrido Alzar *et al.*, Am. J. Phys. **70**, 37 (2001); E. H. El Boudouti *et al.*, J. Phys. Condens. Matter **20**, 255212 (2008).
[6] M. F. Yanik *et al.*, Phys. Rev. Lett. **93**, 233903 (2004).
[7] D. D. Smith *et al.*, Phys. Rev. A **69**, 063804 (2004); L. Maleki *et al.*, Opt. Lett. **29**, 626 (2004).
[8] Y.-F. Xiao *et al.*, Phys. Rev. A **75**, 063833 (2007); Y.-F. Xiao *et al.*, New J. Phys. **10**, 123013 (2008).
[9] See, for example, F. Xia *et al.*, Nat. Photon. **1**, 65 (2007); Y. A. Vlasov *et al.*, Nature (London) **438**, 65 (2005).
[10] S. T. Chu *et al.*, IEEE Photonics Technol. Lett. **11**, 1426 (1999); K. Totsuka *et al.*, Phys. Rev. Lett. **98**, 213904 (2007).
[11] Q. Xu *et al.*, Phys. Rev. Lett. **96**, 123901 (2006); Q. Xu *et al.*, Nature Phys. **3**, 406 (2007).
[12] J. Pan *et al.*, Appl. Phys. Lett. **92**, 103114 (2008).
[13] Y. Akahane *et al.*, Nature (London) **425**, 944 (2003); T. Tanabe *et al.*, Nat. Photon. **1**, 49 (2007); S. Noda *et al.*, Nat. Photon. **1**, 449 (2007).
[14] X. Yang *et al.*, Appl. Phys. Lett. **91**, 051113 (2007); X. Yang and C. W. Wong, Opt. Express **15**, 4763 (2007).
[15] A. Farjadpour *et al.*, Opt. Lett. **31**, 2972 (2006).
[16] A. B. Matsko *et al.*, J. Mod. Opt. **51**, 2515 (2004).
[17] S. Hughes, Phys. Rev. Lett. **98**, 083603 (2007); J. Qian *et al.*, Phys. Rev. A **77**, 023823 (2008).
[18] M. Skorobogatiy *et al.*, Opt. Express **13**, 2487 (2005).
[19] X. Yang *et al.*, Appl. Phys. Lett. **91**, 161114 (2007).
[20] H. A. Haus, *Waves and Fields in Optoelectronics* (Prentice-Hall, Englewood Cliffs, NJ, 1984), Chap. 7, p. 197.